

# Guaranteed-Safe Approximate Reachability via State Dependency-Based Decomposition

Anjian Li<sup>1</sup>, Mo Chen<sup>1</sup>

**Abstract**—Hamilton Jacobi (HJ) Reachability is a formal verification tool widely used in robotic safety analysis for controlled nonlinear systems experiencing adversarial disturbances. Given a target set that represents a set of unsafe states, the Backward Reachable Tube (BRT) specifies the states from which a system is guaranteed to enter the target under the worst-case disturbance; therefore, the complement of the BRT guarantees safety. However, computing BRTs requires state space discretization, which suffers from exponential computational time and space complexity with respect to the state space dimension. Previously, system decomposition and projection techniques have been investigated for tackling this curse of dimensionality, but the trade off between applicability to a wider class of dynamics and degree of conservatism has been challenging. In this paper, we first propose a State Dependency Graph to represent the system dynamics, and then decompose the full system in a way that only dependent states are included in each subsystem, and “missing” states are treated as bounded disturbance. Thus for a large variety of dynamics in robotics, BRTs can be quickly approximated in lower-dimensional chained subsystems, while conservatism is preserved in the right direction to guarantee safety. We demonstrate our method with numerical experiments on the 4D Quadruple Integrator, and the 6D Bicycle, an important car model that has been intractable to analyze to the best of our knowledge.

## I. INTRODUCTION

As the popularity of mobile autonomous systems rapidly grows in daily life, the importance of safety of these systems substantially increases as well. Especially for safe-critical systems like self-driving cars, drones, and etc., collision avoidance is indispensable, since any crash can lead to serious damage to human, other autonomous agents and the environment. Thus, formal verification is urgently needed to analyze safety properties of these systems.

Optimal control and differential game theory are well-studied for safe-critical systems [1]–[4]. These methods are ideal for analyzing controlled nonlinear systems under the influence of adversarial disturbances. One powerful tool for safety verification is reachability analysis, which not only characterizes the safe states of the systems, but also provides safety controllers [5]–[7]. It has been widely used in trajectory planning [8]–[11], air traffic management [12], [13], and multi-agent collision avoidance [14], [15].

When reachability analysis is used for guaranteeing safety, one computes the Backward Reachable Tube (BRT) [16]. In a collision avoidance scenario, given system dynamics and the unsafe states, the BRT represents the states from which reaching the unsafe states is inevitable within a specified time horizon under the worst-case disturbance.

There is a variety of reachability analysis methods. [6], [17] focus on analytic solutions, which are fast to compute, but

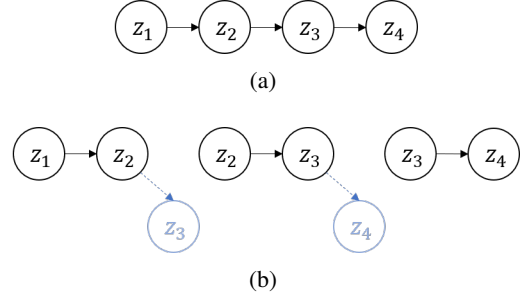


Fig. 1: (a) The State Dependency Graph for 4D Integrator. (b) A decomposed State Dependency Graph for 4D Integrator. The light blue vertices and edges indicate the missing states and their dependencies. Our system method approximates the BRT of the full-dimensional system in Fig. 1(a) by concurrently computing a sequence of BRTs for the subsystems in Fig. 1(b).

require specific types of targets, e.g. polytopes or hyperplanes. Some other techniques have strong assumptions such as linear dynamics [5], [18], or dynamics that do not include any control and disturbance [19]. HJ reachability is the most flexible method that accommodates with nonlinear dynamics and arbitrary shapes of target sets; however, such flexibility requires level set methods [20], [21], in which value functions are stored on grid points in the discretized state space. Such an approach suffers from the curse of dimensionality.

Previously, several approaches have been proposed to reduce the computation burden for HJ reachability. Projection methods have been investigated to approximate BRTs in lower-dimension spaces [22], but it can be difficult to choose which dimensions to project to, and the results can be overly conservative at times. Integrator structures have been analyzed in [23] to reduce dimensionality by one. The state decoupling disturbances method [24] treats certain states as disturbance, thus subsystems can be decoupled and computed on lower-dimensional for goal-reaching problems. An exact system decomposition method [25] has also been used for reducing computation burden without incurring approximation errors. However, this approach is only applicable if there exist self-contained systems, which can sometimes be restrictive.

In this paper, we propose a novel system decomposition method that exploits state dependency information in the system dynamics in a more sophisticated, multi-layered manner compared to previous works. Our approach involves representing the system dynamics using a directed dependency graph, and decomposing the full system into subsystems based on this graph. This is done in a way that allows computation of BRT over-approximations to be tractable yet not overly conservative. A set of lower-dimensional BRTs is computed concurrently: “missing” states in each subsystem are treated

<sup>1</sup>School of Computing Science, Simon Fraser University, Burnaby, BC, Canada, {anjianli, mochen}@sfu.ca

as disturbances, the range of which are bounded by the other BRT approximations being computed.

Our method is applicable to a large variety of system dynamics, especially those with a relatively sparse, “chained” structure. It is easy to combine our method with other decomposition techniques to achieve even more dimensionality reduction. Beyond that, our method also offers a flexible way of adjusting the trade-off between computational complexity and degree of conservatism. This means that our method is adaptable and relevant regardless of the amount of computational resources available.

#### Organization:

- In Section II, we introduce the background on HJ reachability and projection operations of value functions.
- In Section III, we first present how our method decomposes dynamical systems into several smaller subsystems. Then, we discuss how BRT over-approximations can be computed given these subsystems. Finally, we present a proof of correctness, computation complexity analysis, and a discussion on target set selection.
- In Section IV, we present numerical results for the 4D Quadruple Integrator and 6D Bicycle.
- In Section V, we make brief concluding remarks and suggest future research directions.

## II. BACKGROUND

HJ reachability is a powerful tool for guaranteed-safety analysis of nonlinear system dynamics, compatible with arbitrary shapes of target sets, which represent the safe or unsafe states. Given a target set, minimal BRTs can be used to specify the states that will inevitably lead to collision; safety is guaranteed for all states outside of the BRT. In this section, we present the necessary setup for HJ reachability computation, and introduce the projection operations used in our method.

### A. System Dynamics

Let  $z \in \mathbb{R}^n$  represent the state and  $s$  represent time. The system dynamics is described by the following ODE:

$$\dot{z} = \frac{dz}{ds} = f(z, u, d), \quad s \in [s_0, 0], s_0 \leq 0$$

$$u \in \mathcal{U}, d \in \mathcal{D} \quad (1)$$

The  $u(\cdot)$  and  $d(\cdot)$  denote the control function and disturbance function. For any fixed  $u$  and  $d$ , the dynamics  $f : \mathbb{R}^n \times \mathcal{U} \times \mathcal{D} \rightarrow \mathbb{R}^n$  is assumed to be uniformly continuous, bounded and lipschitz continuous; thus, a unique solution to (1) exists given  $u$  and  $d$ .

The solution for (1), or trajectory, is denoted as  $\zeta(s; z, s_0, u(\cdot), d(\cdot)) : [s_0, 0] \rightarrow \mathbb{R}^n$ , which starts from state  $z$  at time  $s_0$  under control  $u$  and disturbance  $d$ .  $\zeta$  satisfies (1) almost everywhere with initial condition:

$$\frac{d}{ds} \zeta(s; z, s_0, u(\cdot), d(\cdot)) = f(\zeta(s; z, s_0, u(\cdot), d(\cdot)), u(s), d(s)),$$

$$\zeta(s_0; z, s_0, u(\cdot), d(\cdot)) = z. \quad (2)$$

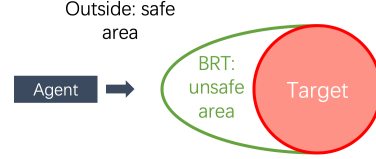


Fig. 2: An example the target and the BRT. To avoid the target, the agent should stay outside of the BRT.

The control and disturbance have opposing objectives, and are modeled as opposing players in a differential game. Following [2], we let  $d(\cdot) = \gamma[u](\cdot)$ , where  $\gamma$  is drawn from only nonanticipative strategies.

### B. Hamilton-Jacobi Reachability

Given a target  $\mathcal{T}$  to avoid, the BRT is the set of states from which there exists a disturbance such that entering the target during the time horizon of duration  $|s_0|$  is inevitable despite the best control. This is illustrated in Fig. 2.

Therefore, agents can remain safe for some time horizon by staying outside of the BRT of the corresponding duration. The definition of the minimal BRT  $\bar{\mathcal{A}}(s)$  is as follows:

$$\bar{\mathcal{A}}(s) = \{z : \exists d(\cdot) \in \mathbb{D}, \forall u(\cdot) \in \mathbb{U}, \exists s \in [s_0, 0], \zeta(s; z, s_0, u(\cdot)) \in \mathcal{T}\} \quad (3)$$

In the HJ formulation, the target set is represented as the sub-level set of some function  $l(z)$ , where  $z \in \mathcal{T} \Leftrightarrow l(z) \leq 0$ . Then, the HJ formulation of the reachability problem becomes the differential game problem below:

$$V(z, s) := \min_{d(\cdot)} \max_{u(\cdot)} \min_{s \in [s_0, 0]} l(\zeta(0; z, s, u(\cdot), d(\cdot))) \quad (4)$$

The value function  $V(z, s)$  can be obtained as the viscosity solution of the following HJ partial differential equation: (4):

$$\min\{D_s V(z, s) + H(z, \nabla V(z, s)), V(z, 0) - V(z, s)\} = 0,$$

$$V(z, 0) = l(z), s \in [s_0, 0] \quad (5)$$

where

$$H(z, \nabla V(z, s)) = \min_{d(\cdot)} \max_{u(\cdot)} \nabla V(z, s)^\top f(z, u) \quad (6)$$

The level set method [20] is a computation tool to solve (5) in the discretized state space. Recently, toolboxes [26], [27] have been developed to take pre-defined system dynamics and target sets as input, and numerically compute BRTs using the level set method.

### C. Projection

We present two kinds of projection operations that are used to manipulate value functions of BRTs between high dimension spaces and their low dimension subspaces. Let  $V(x, y) : \mathbb{R}^{n_x + n_y} \rightarrow \mathbb{R}$  be a value function in  $n_x + n_y$  dimension space, where  $x \in \mathbb{R}^{n_x}$  and  $y \in \mathbb{R}^{n_y}$ .

Given a BRT represented by  $V(x, y)$ , we define the projected BRT in its  $n_x$  dimension subspace by the value  $W(x) : \mathbb{R}^{n_x} \rightarrow \mathbb{R}$ , where

$$W(x) = \min_y V(x, y) \quad (7)$$

Given  $W(x)$  in  $n_x$ -dimensional space, we define the value function  $V(x, y)$  representing the back projected BRT as

$$V(x, y) = W(x), \quad \forall y \in \mathbb{R}^{n_y}. \quad (8)$$

### III. METHODOLOGY

Reachability analysis relies on an accurate model of the robotic system under consideration, but accurate models tend to be high-dimensional. This often makes HJ reachability intractable due to the curse of dimensionality.

In this section, we first present a novel method to decompose the dynamical system in (1) into several coupled subsystems, based on a State Dependency Graph. Then, we provide an algorithm for computing BRTs with these subsystems. Finally, we provide the proof of correctness of our method, analyze its computational time and space complexity, and discuss the constraints for target sets.

#### A. System decomposition

1) **State Dependency Graph:** Let  $S$  be the set of states,  $S = \{z_i\}_{i=1}^n$ . We first define the notion of “state dependency”: for some states  $z_i, z_j \in S$ ,  $z_i$  depends on  $z_j$  in  $f(z, s)$  means  $\frac{dz_i}{ds}$  is a function of  $z_j$ .

In order to clarify these dependency relationships between each state of  $S$  in system dynamics  $f(z, s)$ , we define a directed State Dependency Graph  $G = (S, E)$  based on the system dynamics. The set of vertices is denoted  $S$ , and contains all state variables. If some state component  $z_i \in S$  depends on  $z_j$  in  $f(z, s)$ , then the graph  $G$  would have a directed edge from  $z_i$  to  $z_j$ ,  $(z_i, z_j) \in E$ .

Often, high-dimensional dynamics contain chains of integrators. Thus, we consider a running example: 4D Quadruple Integrator, whose states  $z = (z_1, z_2, z_3, z_4) \in \mathbb{R}^4$ . The dynamics are as follows:

$$\begin{bmatrix} \dot{z}_1 \\ \dot{z}_2 \\ \dot{z}_3 \\ \dot{z}_4 \end{bmatrix} = \begin{bmatrix} z_2 + d \\ z_3 \\ z_4 \\ u \end{bmatrix}, \quad u \in \mathcal{U}, d \in \mathcal{D}, \quad (9)$$

where  $u$  and  $d$  denote the control and disturbance. For the system in (9),  $S = \{z_1, z_2, z_3, z_4\}$ ,  $E = \{(z_1, z_2), (z_2, z_3), (z_3, z_4)\}$ , and its State Dependency Graph  $G = (V, E)$  is shown in Fig. 1(a).

2) **Choosing coupled subsystems:** Given the State Dependency Graph  $G$  and the computational space constraint that each subsystem can be at most  $p$ -dimensional, we can decompose the full system  $S$  with state  $z$  into several coupled subsystems  $S_1, S_2, \dots, S_m$  with subsystem states denoted as  $x_1, x_2, \dots, x_m$  respectively, with the following properties:

- In every subsystem, each state should depend on or be depended on by at least one other state.
- Every subsystem should include no more than  $p$  states.

- Subsystems should be chained: each subsystem should share at least one state with another subsystem.

As a result, the decomposed system is represented by connected subgraphs of  $G$  each representing a subsystem. Let  $S_i$  be the set of state variables included in the  $i^{th}$  subsystem, and let  $S_i^c$  be the set of states that not included in  $i^{th}$  subsystem, i.e.  $\forall i, S_i^c = S \setminus S_i$ .

For example, suppose that one requires the maximum dimensionality of subsystems to be two,  $p = 2$ . We can decompose the 4D Quadruple Integrator into 3 subsystems with  $S_1 = \{z_1, z_2\}$ ,  $S_2 = \{z_2, z_3\}$ ,  $S_3 = \{z_3, z_4\}$ . In terms of the subsystem state variables, we have  $x_1 = (z_1, z_2)$ ,  $x_2 = (z_2, z_3)$ , and  $x_3 = (z_3, z_4)$ . The result of the decomposition is shown in Eq. (10), and the corresponding State Dependency Graph representing subsystems is illustrated in Fig. 1(b).

$$\begin{aligned} S_1 : x_1 &= \begin{bmatrix} \dot{z}_1 \\ \dot{z}_2 \end{bmatrix} = \begin{bmatrix} z_2 + d \\ z_3 \end{bmatrix}, d \in \mathcal{D}, z_3(s) \in R_{z_3}(z_2, s) \\ S_2 : x_2 &= \begin{bmatrix} \dot{z}_2 \\ \dot{z}_3 \end{bmatrix} = \begin{bmatrix} z_3 \\ z_4 \end{bmatrix}, z_4(s) \in R_{z_4}(z_3, s) \\ S_3 : x_3 &= \begin{bmatrix} \dot{z}_3 \\ \dot{z}_4 \end{bmatrix} = \begin{bmatrix} z_4 \\ u \end{bmatrix}, u \in \mathcal{U} \end{aligned} \quad (10)$$

In each subsystem, there may be zero or more missing state components. For the 4D Quadruple Integrator, the missing state of  $S_1$  is  $z_3$  since  $z_3 \notin S_1$ . To guarantee safety, we assume the worst case for the missing states by treating them as virtual disturbances, which leads to an over-approximated BRT that is conservative in the right direction [22].

To avoid excessive conservatism, the virtual disturbances are not drawn from the whole computation range. Instead, we will compute the value functions of all the subsystems concurrently to able to access the up-to-date approximate BRTs of other subsystems. Since all the subsystems are chained, one can determine the bounds of virtual disturbances by searching the value functions of other subsystems that contain the corresponding state.

Formally, consider some subsystem  $S_i$ , and let  $R_{z_j}(x_i, s)$  denote the range of the missing state  $z_j \notin S_i$ . Suppose  $z_j \in S_k$  with  $S_k$  being chained with  $S_i$ ,  $S_k \cap S_i \neq \emptyset$ . Note that  $k$  is not unique, as  $z_j$  may be a state of many different subsystems. Furthermore, let  $W_k(x_k, s)$  be the value function for the subsystem  $S_k$  at the time  $s$ . Then,  $R_{z_j}(x_i, s)$  is determined from  $W_k(x_k, s)$  as follows:

$$\begin{aligned} R_{z_j}(x_i, s) &= \{z_j | W_k(x_k, s) \leq 0, \\ &\quad \forall k \text{ such that } z_j \in S_k \wedge S_k \cap S_i \neq \emptyset\} \end{aligned} \quad (11)$$

Besides reducing dimensionality, our method also provides a simple way to adjust the trade off between computational burden and degree of conservatism. Depending on different requirements for computational time, computational space, and approximation accuracy, one can easily switch between having higher-dimensional subsystems for which BRTs are slower to compute but more accurate, and having lower-dimension subsystems for which BRTs are faster to compute but more conservative.

TABLE I: Decomposition suggestions for 5D Car and 6D Planar Quadrotor

System configuration	System dynamics	State Dependency Graph	Decomposed State Dependency Graph	Time and space
5D Car $(x, y)$ -position $\theta$ - heading $v$ - speed $\omega$ - turn rate $u_a$ - accel. control $u_\alpha$ - ang. accel. control	$\begin{bmatrix} \dot{x} \\ \dot{y} \\ \dot{\theta} \\ \dot{v} \\ \dot{\omega} \end{bmatrix} = \begin{bmatrix} v \cos \theta \\ v \sin \theta \\ \omega \\ u_a \\ u_\alpha \end{bmatrix}$			Ground truth: both $O(k^5)$ Decomposition: $O(k^4)$ and $O(k^3)$
6D Planar Quadrotor $(x, y)$ -position $(v_x, v_z)$ - velocity $\theta$ - pitch $\omega$ - pitch rate $u_T$ - thrust control $u_\tau$ - ang.accel.control	$\begin{bmatrix} \dot{x} \\ \dot{z} \\ \dot{v}_x \\ \dot{v}_z \\ \dot{\theta} \\ \dot{\omega} \end{bmatrix} = \begin{bmatrix} v_x \\ v_z \\ -u_T \sin \theta \\ u_T \cos \theta - g \\ \omega \\ u_\tau \end{bmatrix}$			Ground truth: both $O(k^6)$ Decomposition: $O(k^4)$ and $O(k^3)$

**Algorithm 1** Approximating full-dimensional BRTs with chained subsystems

**Require:** System dynamics  $f(z, u, d)$  described as (1) and a function  $l(z)$  representing the target set  $\mathcal{T}$

- 1: Initialize the full-dimensional final time value function  $V(z, 0)$  as (5)
- 2: Decompose the entire system into chained subsystems  $S_1, S_2, S_3, \dots, S_n$ , based on Section III-A
- 3: Initialize the final time value functions  $W_i(x_i, 0)$  for each subsystem  $S_i$  based on (12)
- 4: **for** ( $s = 0$ ;  $s \geq s_0$ ;  $s = s - \Delta s$ ) **do**
- 5:     **for each subsystem**  $S_i$
- 6:         Find the range  $R_{z_j}(x_i, s)$  of the missing states  $z_j$  based on (11)
- 7:         Obtain  $W_i(x_i, s)$  by solving the HJ equation in (13)
- 8:     **end for**
- 9: Obtain the approximated  $V(z, s_0)$  based on (15)
- 10: Obtain the approximated full-dimensional BRT from the zero sub-level set of  $V(z, s_0)$
- 11: For any time  $s$ , obtain the optimal controller as (16) and (17)

Although in general it may not be possible to decompose arbitrary dynamical systems in the form of (1) in a way that saves computation time, our approach is very flexible and can often successfully decompose many realistic system dynamics. We demonstrate the method by decomposing the high-dimensional, tightly coupled 6D Bicycle in Section IV-B. We also present decomposition suggestions for two other common system dynamics, 5D car [28] and 6D planar quadrotor [10], in TABLE I.

### B. Backward Reachable Tube Computation

We now present the procedure for over-approximating BRTs with low-dimensional chained subsystems  $S_1, \dots, S_m$ . Given the target set  $\mathcal{T}$  and the corresponding final condition to the HJ PDE (5),  $l(z) = V(z, 0)$ , we project the full-dimensional BRT onto the subspace of each subsystem  $S_i$ , and initialize the final time value function  $W_i(x_i, 0)$  for the subsystem  $S_i$  using the projection operation in (7) as follows:

$$W_i(x_i, 0) = \min_{z_i \in S_i^c} V(z, 0) \quad (12)$$

Then, given  $W_i(x_i, t)$  for some  $t$ , we compute the value function  $W_i(x_i, s)$  backwards in time for each subsystem following standard HJ PDE theory and numerical methods, while treating missing variables as virtual disturbances with

appropriate bounds. For each time step  $s \in [t - \Delta s, t]$ ,  $W_i(x_i, s)$  is the viscosity solution of the following HJ partial differential equation:

$$\min\{D_s W_i(x_i, s) + H(x_i, \nabla W_i(x_i, s)), W_i(x_i, 0) - W_i(x_i, s)\} = 0, \quad (13)$$

The Hamiltonian is given by

$$H(x_i, \nabla W_i(x_i, s)) = \min_{\substack{d \in \mathcal{D} \\ z_k \in R_{z_k}(x_i, s), \\ \forall z_k \in S_i^c}} \max_{u \in \mathcal{U}} \sum_{z_j \in S_i} \frac{\partial W_i(x_i, s)}{\partial z_j} \cdot \frac{\partial z_j}{\partial s} \quad (14)$$

where  $R_{z_i}(x_i, s)$  is the range of missing states  $\{z_k\}$  given in (11).

This procedure starts at  $t = -\Delta s$ , and finishes when  $W_i(x_i, s_0)$  is obtained. Finally, we take the maximum of all the  $W_i(x_i, s_0)$  as the over-approximation of the full-dimensional initial time  $V(z, s_0)$ :

$$V(z, s_0) = \max_i W_i(x_i, s_0) \quad (15)$$

In general for any time  $s$ , we also have

$$V(z, s) = \max_i W_i(x_i, s). \quad (16)$$

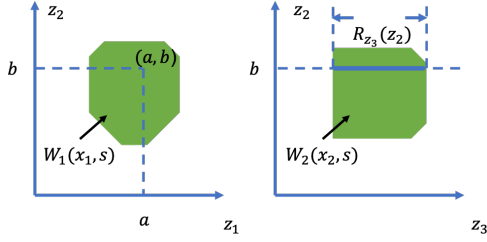


Fig. 3: Searching missing states for 4D Quadruple Integrator. Left: a BRT described by  $W_1(x_1, s)$  for subsystem  $S_1$ . Right: a BRT described by  $W_2(x_2, s)$  for subsystem  $S_2$ . When solving on the grid point of  $(z_1, z_2) = (a, b)$  in subsystem  $S_1$  at time  $s$ , we find the range of missing state  $R_{z_3}(z_2, s)$  inside the BRT from subsystem  $S_2$ .

The optimal controller is given by

$$u^*(s) = \operatorname{argmax}_u \nabla V(z, s)^\top f(z, u). \quad (17)$$

The computation process is summarized in **Algorithm 1**.

Consider our running example, the 4D Quadruple Integrator in (9) and its subsystems in (10). In particular, consider the BRT computation for subsystem  $S_1 = \{z_1, z_2\}$ . At the time  $s$ , the HJ equation in (13) for subsystem  $S_1$  becomes

$$\min \left\{ \frac{\partial W_1(x_1, s)}{\partial s} + \min_{z_3 \in R_{z_3}(z_2, s)} \left( \frac{\partial W_1(x_1, s)}{\partial z_1} z_2 + \frac{\partial W_1(x_1, s)}{\partial z_2} z_3 \right), W_1(x_1, 0) - W_1(x_1, s) \right\} = 0 \quad (18)$$

Here for the subsystem  $S_1$  in (10), given  $z_2$ , we are able to find the range of  $z_3$  in the subsystem  $S_2$ . Let  $W_2(x_2, s)$  be the value function for the subsystem  $S_2$  at the time  $s$ , the range of  $z_3$  given  $z_2$  will be defined as  $R_{z_3}(z_2, s)$ :

$$R_{z_3}(z_2, s) := \{z_3 | W_2(x_2, s) \leq 0\} \quad (19)$$

A graphical interpretation of (19) is in Fig. 3. For a specific grid point of  $(z_1, z_2) = (a, b) \in \mathbb{R}^2$  in the subsystem  $S_1$ , the range of the missing state  $R_{z_3}(z_2, s)$  can be drawn from the subsystem  $S_2$  with the corresponding  $z_2 = b$ .

### C. Proof and Discussions

1) **Proof of Correctness:** In this section, we show that the BRT generated from our method is an over-approximation of the true BRT obtained from (5). Let  $V_i(z, s)$  denote the full-dimensional value function that back projected from  $W_i(x_i, s)$  at the time  $s$ , based on the projection operation in (8):

$$V_i(z, s) = W_i(x_i, s), \forall z_i \in S_i^c \quad (20)$$

Because at any time  $s$ , we maximize over  $W_i(x_i, s)$  to obtain the over-approximation, to prove the following Theorem 1 is sufficient to prove that each approximate value function  $V_i$  is no larger than the true value function  $V$ .

**Theorem 1:** For any subsystem  $S_i$  at any time step  $s \in [t - \Delta s, t]$ ,  $V_i(z, s) \leq V(z, s)$

**Proof:** We prove this by mathematical induction. For any subsystem  $S_i$ , we first show that the Theorem at final time  $s = 0$  is true. Then we prove that for any time step

$s \in [t - \Delta s, t]$ , if  $V_i(z, t) \leq V(z, t)$ , we will have  $V_i(z, t - \Delta s) \leq V(z, t - \Delta s)$ .

At the final time  $s = 0$ ,  $W_i(x_i, 0)$  is initialized as (12) and  $V_i(z, s)$  is initialized as (20), thus trivially we have

$$V_i(z, 0) \leq V(z, 0). \quad (21)$$

For any time step  $s \in [t - \Delta s, t]$ ,  $V(z, s)$  is the viscosity solution of (5) with final value  $V(z, t)$ . Let  $\tilde{V}_i(z, t - \Delta s)$  be the viscosity solution of (5) with final value  $V_i(z, t)$ . Since  $V_i(z, t) \leq V(z, t)$ , we have

$$\tilde{V}_i(z, t - \Delta s) \leq V(z, t - \Delta s) \quad (22)$$

Let  $W_i(x_i, s)$  be the viscosity solution of (13) at  $s \in [t - \Delta s, t]$  with final value  $W_i(x_i, t)$ . When solving  $W_i(x_i, t - \Delta s)$ , the Hamiltonian  $H(x_i, \nabla W_i(x_i, s))$  is computed as (14). For comparison, when solving  $\tilde{V}_i(z, t - \Delta s)$ , the Hamiltonian  $H(z, \nabla \tilde{V}_i(z, s))$  is computed as (6).

Because  $V_i(z, t)$  is back projected from  $W_i(x_i, t)$  as (20), in  $H(z, \nabla V_i(z, s))$  we have  $\frac{\partial V_i(z, t)}{\partial z_i} = 0, \forall z_i \in S_i^c$ . In addition, missing states are treated as disturbances in  $H(x_i, \nabla W_i(x_i, s))$ , so  $H(x_i, \nabla W_i(x_i, s)) = \min_{\forall z_i \in S_i^c} H(z, \nabla \tilde{V}_i(z, s))$ . Therefore,

$$H(x_i, \nabla W_i(x_i, s)) \leq H(z, \nabla \tilde{V}_i(z, s)), \forall z_i \in S_i^c. \quad (23)$$

Thus we obtain

$$W_i(x_i, t - \Delta s) \leq \tilde{V}_i(z, t - \Delta s), \forall z_i \in S_i^c. \quad (24)$$

Because  $V_i(z, t - \Delta s)$  is back projected from  $W_i(x_i, t - \Delta s)$  as (20), we have

$$V_i(z, t - \Delta s) \leq \tilde{V}_i(z, t - \Delta s). \quad (25)$$

Finally, for any time step  $s \in [t, t - \Delta s]$ , we combine (22) and (25) and obtain

$$V_i(z, t - \Delta s) \leq V(z, t - \Delta s). \quad (26)$$

■

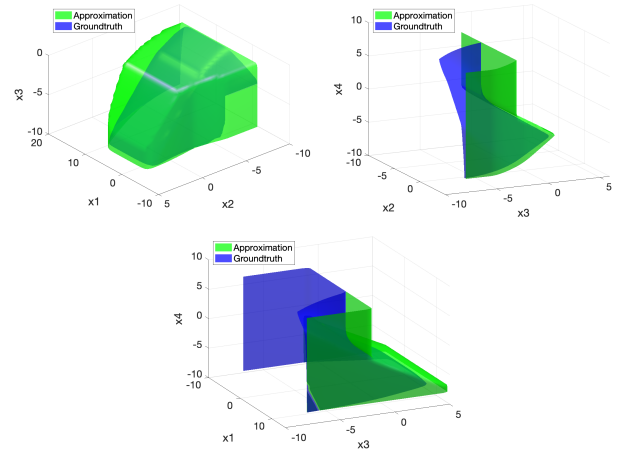


Fig. 4: Comparison of ground truth BRTs (blue) and our approximated BRTs (green) for 4D Quadruple Integrator at  $s = -1$ . From top left, top right to bottom are 3D slices at  $z_4 = -2, z_1 = 2.6, z_2 = -4.2$ . There are few numerical errors.



2) **Computation complexity:** Let  $k$  be the number of grid points in each dimension for the numerical computation. The computational space complexity is determined by the largest dimension of subsystems. If each subsystem  $S_i$  has  $N_i$  states,  $k^{\max_i N_i}$  grid points are needed to store the value function. Overall, the space complexity is  $O(k^{\max_i N_i})$ .

For computation time, there are two non-trivial parts: solving the HJ PDE and searching the missing states. The HJ PDE is solved on a grid with  $O(k^{N_i})$  grid points. If this search is done over an  $M_i$ -dimensional grid for subsystem  $S_i$ , then these nested loops have a time complexity of  $O(k^{N_i+M_i})$ . Overall, all, the upper limit of the computation time will be the longest time among all subsystems,  $O(k^{\max_i \{N_i+M_i\}})$ . The computational complexity of specific numerical examples can be found in Section IV.

3) **Target sets:** Our decomposition technique has two constraints of the target sets. First, for each subsystem, there should be a clear boundary of the target, so that the subsystem value function can provide a virtual disturbance bound to other subsystems. Second, the entire target should be the intersections of all targets from each subsystem. Because each subsystem may share controls or disturbances, according to [25], only BRT and target set intersections lead to conservative approximations.

#### IV. NUMERICAL EXPERIMENTS

We demonstrate our method on the running example, 4D Quadruple Integrator, and on the higher-dimensional, heavily coupled 6D Bicycle model [10]. For the 4D Quadruple Integrator, we compare the approximate BRT computed using our method to ground truth BRT obtained from the full-dimensional computation, showing that our method maintains the safety guarantee without introducing much conservatism. For 6D Bicycle, we present for the first time a conservative but still practically useful BRT in a realistic simulated autonomous driving scenario. To the best of our knowledge, this was previously intractable. All the experiment are implemented on an AMD Ryzen 9 3900X 12-Core Processor with ToolboxLS [26] and helperOC toolbox.

##### A. 4D Quadruple Integrator

The system dynamics of the 4D Quadruple Integrator is given in (9). Using our method, we decompose the system into subsystems shown in (10). Starting from the target set  $\mathcal{T}$  in (27), and we compute the approximate BRT for for a time horizon of 1.0 second.

$$\mathcal{T} := \{(z_1, z_2, z_3, z_4) \mid -6 < z_1 < 6, z_2 < -4, z_3 < -2\} \quad (27)$$

In Fig. 4, we visualize the 4D BRT through 3D slices at the initial time  $s = -1.0$ . From top left, top right to bottom, our approximated BRTs (green) and the ground truth BRTs (blue) are shown, at the slices of  $z_4 = -2$ ,  $z_1 = 2.6$ , and  $z_2 = -4.2$  respectively. The results show that our approximated BRTs are similar in shape to the ground truth BRT while being a little bigger, which indicates that our results are conservative in the right direction: if a state is outside of the approximate

BRT, it is guaranteed to be safe. There are few exceptions due to numerical errors.

For the 4D Quadruple Integrator, the largest subsystem has two states, so the computation space is  $O(k^2)$ . When solving subsystems  $S_1$  and  $S_2$ , we all should search the missing state from another one dimension grid in subsystem  $S_2$  and  $S_3$ , with fixed states  $z_2$  and  $z_3$ . Thus, the computation time is  $O(k^3)$ . To compare, computing ground truth BRTs for 4D Quadruple Integrator in the full dimension space will cost  $O(k^4)$  both on space and time.

In our experiment, it takes 2.5 seconds to compute approximation from decomposition, while it takes 420 seconds to compute the ground truth in full dimension.

##### B. 6D Bicycle

We now examine the proposed decomposition method on a practical example involving the 6D Bicycle model, and illustrate the utility of our method on decomposing high-dimensional system and heavily coupled systems. To the best of our knowledge, this is the first practically usable minimal BRT computation for 6D Bicycle, a model widely used to approximate the behaviour of four-wheeled vehicles such as autonomous cars.

1) **Problem Setup:** The system dynamics is given in (28).  $X$  and  $Y$  denote position in the global frame,  $\psi$  denotes the orientation angle with respect to the  $X$  axis<sup>1</sup>,  $v_x$  and  $v_y$  denote the longitudinal and lateral velocities, and  $\omega$  denotes the angular speed. The controls are  $\delta_f$  and  $a_x$ , which represent the steering angle and longitudinal acceleration, respectively.

$$\begin{bmatrix} \dot{X} \\ \dot{Y} \\ \dot{\psi} \\ \dot{v}_x \\ \dot{v}_y \\ \dot{\omega} \end{bmatrix} = \begin{bmatrix} v_x \cos \psi - v_y \sin \psi \\ v_x \sin \psi + v_y \cos \psi \\ \omega \\ \omega v_y + a_x \\ -\omega v_x + \frac{2}{m}(F_{c,f} \cos \delta_f + F_{c,r}) \\ \frac{2}{I_z}(l_f F_{c,f} - l_r F_{c,r}) \end{bmatrix} \quad (28)$$

To decompose 6D Bicycle, we hope to achieve the best accuracy within the current computation resources, hence we set the space and time limits to be  $O(k^4)$ . Based on the State Dependency Graph for 6D Bicycle in Fig. 5(a), we choose the subsystems in (29) with the corresponding decomposed State Dependency Graph shown in Fig. 5(b), which requires  $O(k^3)$  space and  $O(k^4)$  time complexity.

$$\begin{aligned} x_1 &= (X, v_x, v_y), x_2 = (Y, v_x, v_y), x_3 = (X, \psi), \\ x_4 &= (Y, \psi), x_5 = (v_x, v_y, \omega), x_6 = (\psi, \omega) \end{aligned} \quad (29)$$

We design the target set  $\mathcal{T}$  with respect to  $X$ ,  $Y$ ,  $\psi$  and  $v_x$  in (30). This situation can be represented as a one way road surrounded by an open area in a parking lot as Fig. 6. In the one way road, only a positive forward speed and a forward orientation range is allowed<sup>2</sup>.

$$\mathcal{T} := \{(X, Y, \psi, v_x, v_y, \omega) \mid -6 < X < 6, -2 < Y < 2, \psi < 7\pi/4, v_x < 0\} \quad (30)$$

<sup>1</sup>Computation bound for  $\psi$  is  $[\pi/4, 9\pi/4]$

<sup>2</sup>Combined with the computation bound, the safe orientation range are  $[-\pi/4, \pi/4]$

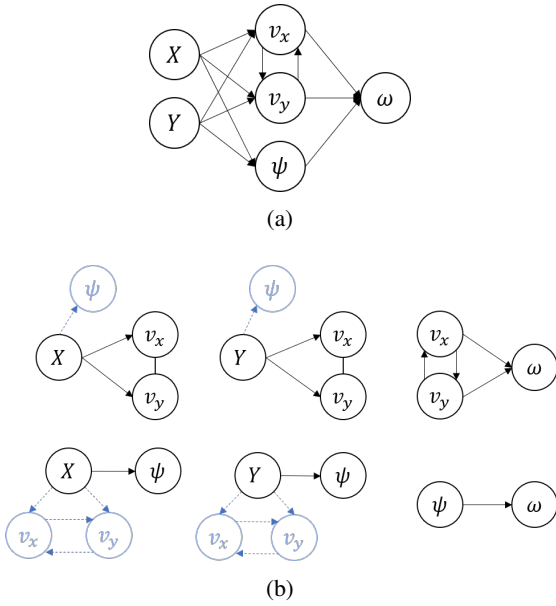


Fig. 5: (a) The State Dependency Graph for 6D Bicycle. (b) A decomposed State Dependency Graph for 6D Bicycle. The light blue vertices and edges indicate the missing states and their dependency.

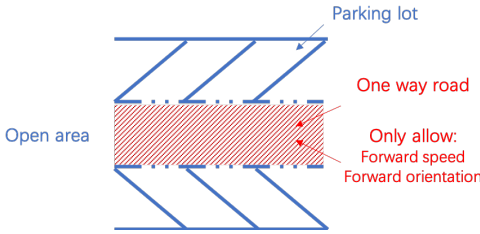


Fig. 6: A target set example for 6D Bicycle. Inside a parking lot, there is a one-way road surrounded by open areas, where only a positive forward speed and a forward orientation range are allowed.

We compute the BRT for a time horizon of 2 seconds.

2) **BRT Result:** To visualize the 6D BRT at  $t = -2.0$ , we present several 3D slices in Fig. 7 and Fig. 8.

Fig. 7 shows the BRT at the slice of  $\psi = \pi/4, \omega = -1.1$ ,  $v_y = 0$  (left) and 18 (right), indicating the range of  $v_x$  to avoid for different  $X$  and  $Y$ . As shown, the farther from the area  $\{(x, y) | -6 < x < 6, -2 < y < 2\}$ , the smaller set of  $v_x$  needs to be avoided to maintain safety. This is because if the agent is far from the unsafe positions, it has more time and space to slow down and adjust  $v_x$ . In comparison, in the right plot, the agent has a larger  $v_y = 18$ , and thus has a larger BRT in  $v_x$  to avoid, especially in the  $Y$  direction.

Fig. 8 shows the BRTs at the slice of  $\psi = \pi/4, v_x = 18$ ,  $v_y = 3$  (left) and 18 (right), indicating the range for  $\omega$  to avoid on the computation area of  $X$  and  $Y$ . We get similar results as above: the farther from the target area  $\{(x, y) | -6 < x < 6, -2 < y < 2\}$ , the smaller sets of  $\omega$  one needs to avoid, due to more time and space for adjustment. In the right plot,  $v_y = 18$ , a larger value; thus more distance is needed to adjust  $\psi$ . As a result, the BRT is larger.

In our experiment, it takes 17 minutes to compute the approximated BRT with the decomposition method.

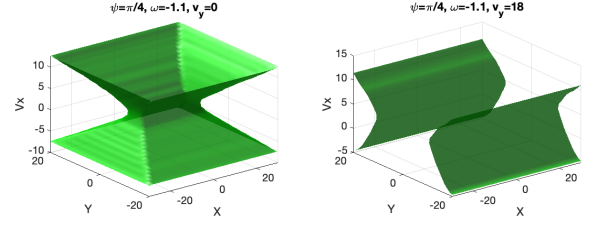


Fig. 7: 3D slices of  $(X, Y, v_x)$  from 6D BRT at  $s = -2$ . Left: slice at  $\psi = \pi/4, \omega = -1.1, v_y = 0$ . Right: slice at  $\psi = \pi/4, \omega = -1.1, v_y = 18$

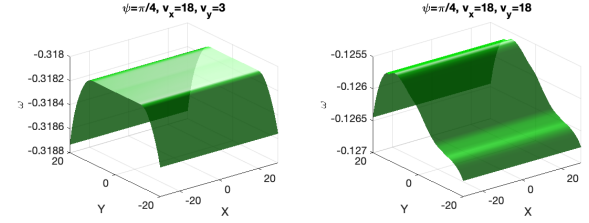


Fig. 8: 3D slices of  $(X, Y, \omega)$  from 6D BRT at  $s = -2$ . Left: slice at  $\psi = \pi/4, v_x = 18, v_y = 3$ . Right: slice at  $\psi = \pi/4, v_x = 18, v_y = 18$

3) **Safety-Preserving Trajectories:** In Figs. 9 and 10, we present the evolution of the BRT over time, and illustrate that trajectories synthesized using Eq. (17) are guaranteed safe when starting outside the approximated BRTs, and may enter the targets when starting inside the approximated BRTs.

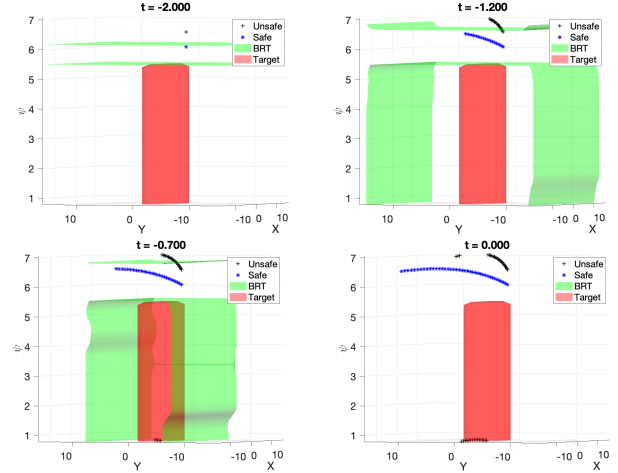


Fig. 9: Comparison of a safe trajectory (blue) and an unsafe trajectory (black) of 6D Bicycle in  $(X, Y, \psi)$  space within the time horizon of 2s. The safe trajectory starts from outside the BRT (green), and successfully avoids all BRTs and the targets (red) within 2s. The unsafe trajectory starts from inside the BRT and finally hits the target from bottom.

In Fig. 7, we present the trajectories in  $(X, Y, \psi)$  space. The safe initial condition (blue) starts from outside the BRT (green), while the unsafe one (black) starts inside. The initial states of  $(v_x, v_y, \omega) = (-10, 1, 0.8)$  are the same for both agents. As time moves forward, the blue trajectory can always stay outside of the BRT at the corresponding time, and avoids the target (red) during the time horizon of two seconds. However, the unsafe trajectory enters the target from the

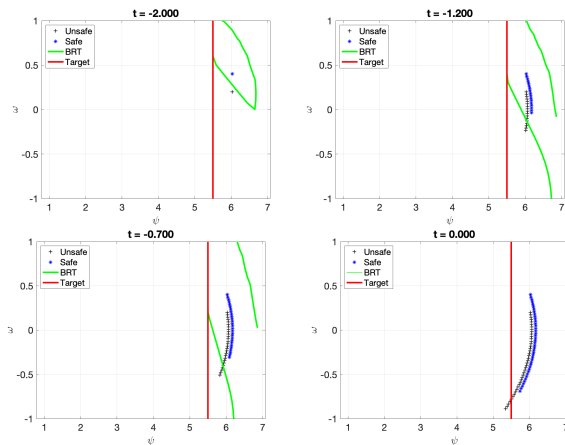


Fig. 10: Comparison of a safe trajectory (blue) and an unsafe trajectory (black) of 6D Bicycle in  $(\omega, \psi)$  space within the time horizon of 2s. The safe trajectory starts from outside of the BRT (green), and successfully avoids all BRTs and the obstacle (red) within two seconds. The unsafe trajectory starts from inside the BRT and finally hits the target from the right side.

bottom of the plot at  $s = -0.8$  (the  $\psi$  dimension is periodic).

In Fig. 8, we present the trajectories in  $(\omega, \psi)$  space. The initial states  $(X, Y, v_x, v_y) = (10, 0, -6, 1)$  are the same for both agents. In the same setting, the safe trajectory (blue) can stay outside the BRT (green) and the target (red) within time horizon of two seconds, but the unsafe trajectory (black) enters the target from right side at  $s = -0.2$ .

## V. CONCLUSION

We propose a decomposition method that largely alleviates the computation complexity for approximating minimal BRTs, without introducing much conservatism. Our method has a superior advantage of solving sparse, high-dimensional integrator, and is able to handle a large variety of nonlinear system dynamics. We also provide a simple way of making trade-off between computation space, speed and performance, which will benefit when more computation resources gained.

In the future, we are interested in investigating techniques that allow under-approximation of BRTs, so that more maximal BRTs will be tractable. Besides, we hope to explore more techniques such as in [29] to overcome the constraints for target sets when computing minimal BRTs.

## REFERENCES

- [1] E. Barron, "Differential games with maximum cost," *Nonlinear analysis: Theory, methods & applications*, vol. 14, no. 11, pp. 971–989, 1990.
- [2] I. M. Mitchell, A. M. Bayen, and C. J. Tomlin, "A time-dependent hamilton-jacobi formulation of reachable sets for continuous dynamic games," *IEEE Trans. Autom. control*, vol. 50, no. 7, pp. 947–957, 2005.
- [3] K. Margellos and J. Lygeros, "Hamilton-jacobi formulation for reach-avoid differential games," *IEEE Trans. Autom. control*, vol. 56, no. 8, pp. 1849–1861, 2011.
- [4] O. Bokanowski and H. Zidani, "Minimal time problems with moving targets and obstacles," *IFAC Proceedings Volumes*, vol. 44, no. 1, pp. 2589–2593, 2011.
- [5] A. B. Kurzhanski and P. Varaiya, "On ellipsoidal techniques for reachability analysis. part ii: Internal approximations box-valued constraints," *Optimization methods and software*, vol. 17, no. 2, pp. 207–237, 2002.

- [6] G. Frehse, C. Le Guernic, A. Donzé, S. Cotton, R. Ray, O. Lebeltel, R. Ripado, A. Girard, T. Dang, and O. Maler, "Spaceex: Scalable verification of hybrid systems," in *Int. Conf. on Computer Aided Verification*, 2011.
- [7] M. Althoff and B. H. Krogh, "Reachability analysis of nonlinear differential-algebraic systems," *IEEE Transactions on Automatic Control*, vol. 59, no. 2, pp. 371–383, 2013.
- [8] C. Parzani and S. Puechmorel, "On a hamilton-jacobi-bellman approach for coordinated optimal aircraft trajectories planning," *Optimal Control Applications and Methods*, vol. 39, no. 2, pp. 933–948, 2018.
- [9] S. L. Herbert, M. Chen, S. Han, S. Bansal, J. F. Fisac, and C. J. Tomlin, "Fastrack: a modular framework for fast and guaranteed safe motion planning," in *Proc. IEEE Conf. on Decision and Control*, 2017.
- [10] S. Singh, M. Chen, S. L. Herbert, C. J. Tomlin, and M. Pavone, "Robust tracking with model mismatch for fast and safe planning: an sos optimization approach," *arXiv preprint arXiv:1808.00649*, 2018.
- [11] B. Landry, M. Chen, S. Hemley, and M. Pavone, "Reach-avoid problems via sum-of-squares optimization and dynamic programming," in *2018 IEEE/RSSJ Int. Conf. Intelligent Robots and Systems*, 2018.
- [12] M. Chen, Q. Hu, C. Mackin, J. F. Fisac, and C. J. Tomlin, "Safe platooning of unmanned aerial vehicles via reachability," in *Proc. IEEE Conf. Decision and Control*, 2015.
- [13] M. Chen, Q. Hu, J. F. Fisac, K. Akametalu, C. Mackin, and C. J. Tomlin, "Reachability-based safety and goal satisfaction of unmanned aerial platoons on air highways," *AIAA J. Guidance, Control, and Dynamics*, vol. 40, no. 6, pp. 1360–1373, 2017.
- [14] M. Chen, J. C. Shih, and C. J. Tomlin, "Multi-vehicle collision avoidance via hamilton-jacobi reachability and mixed integer programming," in *Proc. IEEE Conf. on Decision and Control*, 2016.
- [15] A. Dhinakaran, M. Chen, G. Chou, J. C. Shih, and C. J. Tomlin, "A hybrid framework for multi-vehicle collision avoidance," in *Proc. IEEE Conf. on Decision and Control*, 2017.
- [16] M. Chen and C. J. Tomlin, "Hamilton-jacobi reachability: Some recent theoretical advances and applications in unmanned airspace management," *Annual Review of Control, Robotics, and Autonomous Systems*, vol. 1, pp. 333–358, 2018.
- [17] M. Althoff, O. Stursberg, and M. Buss, "Computing reachable sets of hybrid systems using a combination of zonotopes and polytopes," *Nonlinear analysis: HHybrid Systems*, vol. 4, no. 2, pp. 233–249, 2010.
- [18] J. N. Maidens, S. Kaynama, I. M. Mitchell, M. M. Oishi, and G. A. Dumont, "Lagrangian methods for approximating the viability kernel in high-dimensional systems," *Automatica*, vol. 49, no. 7, pp. 2017–2029, 2013.
- [19] J. Darbon and S. Osher, "Algorithms for overcoming the curse of dimensionality for certain hamilton-jacobi equations arising in control theory and elsewhere," *Research in the Mathematical Sciences*, vol. 3, no. 1, p. 19, 2016.
- [20] I. Mitchell and C. J. Tomlin, "Level set methods for computation in hybrid systems," in *Int. Workshop on Hybrid Systems: Computation and Control*, 2000, pp. 310–323.
- [21] S. Osher, R. Fedkiw, and K. Piechor, "Level set methods and dynamic implicit surfaces," 2004.
- [22] I. M. Mitchell and C. J. Tomlin, "Overapproximating reachable sets by hamilton-jacobi projections," *J. Scientific Computing*, vol. 19, no. 1-3, pp. 323–346, 2003.
- [23] I. M. Mitchell, "Scalable calculation of reach sets and tubes for nonlinear systems with terminal integrators: a mixed implicit explicit formulation," in *Proc. ACM Int. Conf. on Hybrid systems: computation and control*, 2011.
- [24] M. Chen, S. Herbert, and C. J. Tomlin, "Fast reachable set approximations via state decoupling disturbances," in *Proc. IEEE Conf. on Decision and Control*. IEEE, 2016.
- [25] M. Chen, S. Herbert, M. Vashishtha, S. Bansal, and C. Tomlin, "Decomposition of reachable sets and tubes for a class of nonlinear systems," *IEEE Trans. Autom. Control*, vol. 63, no. 11, pp. 3675–3688, 2018.
- [26] I. M. Mitchell, "A toolbox of level set methods," 2009. [Online]. Available: <http://people.cs.ubc.ca/mitchell/ToolboxLS/index.html>
- [27] K. Tanabe and M. Chen, "Beacels library," 2019. [Online]. Available: <https://github.com/HJReachability/beacels/>
- [28] R. Rajamani, *Vehicle dynamics and control*. Springer Science & Business Media, 2011.
- [29] D. Lee, M. Chen, and C. J. Tomlin, "Removing leaking corners to reduce dimensionality in hamilton-jacobi reachability," in *2019*



*International Conference on Robotics and Automation (ICRA)*. IEEE, 2019, pp. 9320–9326.